Macromolecular Materials and Engineering

Optimization of process-control parameters for the diameter of electrospun hydrophilic polymeric composite nanofibers

--Manuscript Draft--

Manuscript Number:	mame.202100471R2
Article Type:	Research Article
Corresponding Author:	Mohan Edirisinghe, Prof. University College London London, UNITED KINGDOM
Corresponding Author E-Mail:	m.edirisinghe@ucl.ac.uk
Order of Authors:	Fawzan S Alfares, Asst.Prof.
	Ece Guler, Doctoral Researcher
	Hussain Alenezi, Doctoral Researcher
	Muhammet Emin Cam, Assoc.Prof.
	Mohan Edirisinghe, Prof.
Keywords:	nanocomposites; electrospinning; numerical analysis; processing parameters
Section/Category:	
Abstract:	A composite nanofiber composed of three polymers, namely polyvinyl alcohol (PVA)/ polyvinyl pyrrolidone (PVP)/ polyethylene oxide (PEO), was produced. The experiments were constructed using three Design of Experiment (DOE) techniques, Taguchi L9, Taguchi L27, and Screening method. The experiments were verified using the ANOVA method, and later a mathematical model was developed using the regression method. The impact of electrospun processing parameters, namely applied voltage, flow rate, and working distance, on the diameter of nanofibers, were measured. The working distance as a significant factor in controlling the size of the fiber diameter while the applied voltage has the lowest effect on it. As a result of the regression equation, a Genetic algorithm was used to find the optimum variables for the required fiber diameter, which was 156 nm for flow rate= 0.001 mL/h, voltage= 30 kV, and distance= 200 mm with 3% difference from the experimental fiber diameter.
Author Comments:	SEM images in higher resolution are available for Figure S1, which were uploaded as Production Data in attached files, but I couldn't use SEM images in higher resolution for Figure S1 due to max size.
Additional Information:	
Question	Response
Please submit a plain text version of your cover letter here.	19th September 2021 Dr David Huesmann Editor-in-Chief Macromolecular Materials and Engineering Dear David Please find enclosed our revised manuscript entitled "Optimization of process parameters on the diameter of electrospun hydrophilic polymeric composite nanofibers". I want to thank you and the reviewers' for the very helpful comments/suggestions. We have very carefully addressed these (see response) and also checked and polished-up the entire manuscript.

	We look forward to its publication in Macromol. Mater. & Eng. Yours sincerely, Mohan
Do you or any of your co-authors have a conflict of interest to declare?	No. The authors declare no conflict of interest.
Response to Reviewers:	1. Please correct the numbering in Table 2. Response: Firstly, we very much appreciate your supportive comments. All numbers were checked again in Table 2. The numbering is correct because not all the variations were used in the experiment. It can be checked from Table S2. 2. In the 7th paragraph of the "Introduction" section, the authors refer to "most studies" and "more studies", but the references are not included. Please indicate the references to which the studies refer. Response: The references were added to the related sentence.

Response to Reviewers

Reviewer #3

The authors have addressed the points I raised in my review. However, minor inconsistencies have been introduced and minor revision is required before acceptance.

1. Please correct the numbering in Table 2.

Response: Firstly, we very much appreciate your supportive comments. All numbers were checked again in Table 2. The numbering is correct because not all the variations were used in the experiment. It can be checked from Table S2.

2. In the 7th paragraph of the "Introduction" section, the authors refer to "most studies" and "more studies", but the references are not included. Please indicate the references to which the studies refer.

Response: The references were added to the related sentence.

Optimization of process-control parameters for the diameter of electrospun hydrophilic polymeric composite nanofibers

Fawzan S. Alfares, Ece Guler, Hussain Alenezi, Muhammet Emin Cam*, Mohan Edirisinghe*

*Corresponding Authors

Dr. F.S. Alfares, H. Alenezi

Department of Manufacturing Engineering, College of Technological Studies, PAAET, 13092

Kuwait City, Kuwait

E. Guler, Assoc.Prof. M.E. Cam

Department of Pharmacology, Faculty of Pharmacy, Marmara University, Istanbul 34716, Turkey

E. Guler, Assoc.Prof. M.E. Cam, Prof. M. Edirisinghe

Center for Nanotechnology and Biomaterials Application and Research, Marmara University,

Istanbul 34668, Turkey

H. Alenezi, Assoc.Prof. M.E. Cam, Prof. M. Edirisinghe

Department of Mechanical Engineering, University College London, Torrington Place, London

WC1E 7JE, UK

E-mail addresses: muhammet.cam@marmara.edu.tr and m.edirisinghe@ucl.ac.uk

A composite nanofiber composed of three polymers, namely polyvinyl alcohol (PVA)/ polyvinyl pyrrolidone (PVP)/ polyethylene oxide (PEO), was produced. The experiments were constructed using three Design of Experiment (DOE) techniques, Taguchi L_9, Taguchi L_{27}, and Screening method. The experiments were verified using the ANOVA method, and later a mathematical model was developed using the regression method. The impact of electrospun processing parameters,

1

namely applied voltage, flow rate, and working distance, on nanofibers' diameter was measured. The working distance is a significant factor in controlling the size of the fiber diameter, while the applied voltage has the lowest effect on it. As a result of the regression equation, a Genetic algorithm was used to find the optimum variables for the required fiber diameter, which was 156 nm for flow rate= 0.001 mL/h, voltage= 30 kV, and distance= 200 mm with a 3% difference from the experimental fiber diameter.

1. Introduction

Nanofibers represent a new class of materials morphology that belongs to nanotechnology, a type of fiber synthesized on a nanoscale to strengthen or replace polymer matrices.[1] Nanofibers are produced from synthetic and natural polymers. More than 100 types of polymers are used to produce nanofibers, such as chitosan, collagen, polylactic acid, hyaluronic acid, polyurethanes, cellulose, and silk. They have several advantages: small fiber diameter, high permeability, low basis weight, high surface area to volume ratio, porous structure, high water uptake capacity, and high passage of oxygen.[2, 3] Nanofibers are used in several different areas, such as energy storage, cancer therapy, functional materials, drug delivery, stem cell therapy, sensors, filtering, biomedical, protective clothing, optical electronics, tissue engineering, environmental engineering, and wound healing.[4-7]

In healthcare, nanofibers are mostly used to reduce wound-healing time in wound bandages, treat infections in wound areas, and prevent bacterial biofilm formation.[8] Nanofibers are produced using several methods such as electrospinning (ES), phase separation, centrifugal spinning, pressurized gyration, drawing, bi-component extrusion, melt blowing, and template synthesis.[9-11] ES is the most used method to produce nanofibers because it is an easy, simple, and adaptable technique.[12]

ES is a process of spinning with the help of electrostatic forces. This sophisticated and straightforward method produces ultra-thin fibers from a wide range of materials containing polymers, composites, and ceramics.[13] In the ES process, a polymeric solution is pumped by the

2

syringe to the tip of the needle through a Taylor cone and the high voltage from an electrical source causes the interaction of forces (electrostatic and surface tension) on the charged surface of a polymer droplet. When the electric forces exceed the surface tension, the jet from the Taylor cone generates fibers, extending towards the fiber collector, and ultimately, polymer nanofibers solidified on the collector forms a nonwoven mesh.[14, 15] The idea is to use the opposite charge that connects the collector area to the needle, which helps the solution evaporate, solidify, and transform the liquid into a solid phase.[16] The average diameter of the nanofibers produced in the ES process is between 50 nm and 500 nm.[17] Furthermore, this process is preferred in many technological areas such as drug release, battery separators, high efficient air and liquid filters, tissue engineering, sensors, cell culture, hydrogen storages, pH and temperature-responsive materials and actuators, solar cells, protective clothing [18, 19] In addition, it can be combined with other methods (e.g. 3D printing, photolithography) for providing complex movements on a large scale.[20]

Water and organic solvent-based polymers are the preferred materials for solutions. Especially, water-soluble polymers are the most chosen polymers globally due to their non-toxic and non-carcinogenic properties.[21] Moreover, high biocompatibility is key, helping the water-soluble polymers to be incorporated into the body in order to simulate the natural texture.[22, 23]

The selection of a suitable solvent as the carrier of a particular polymer is considered as one of the most critical variables in ES.[24] Usually, the number of polymers mixed in an aqueous solution is two in ES. The present research had produced novel hybrid water-soluble polymeric fibers formed by three - polyvinyl alcohol (PVA), polyvinyl pyrrolidone (PVP), and polyethylene oxide (PEO), being the most preferred polymers in the literature. The composite with polymers reflects the features of hydrophilic polymers in the most effective manner. All three synthetic polymers are non-toxic, biodegradable, and biocompatible. In addition, they can form a good film by forming positive interactions through their hydroxyl groups. Furthermore, PEO can adopt a wide range of changes in molecular weight to form different polymer compounds.[25, 26]

Taguchi is a well-known process optimization method based on multi-step planning, execution, and evaluation of experimental matrix results to determine the best control factors.[27] The Taguchi method orthogonal arrays are a set of experiments, variables, and levels with unique orthogonal array architecture. Using such arrays can determine the number of tests required for a set of factors without losing credibility. Screening design was used as another model in the design of experiments, which refers to an experimental plan to find the critical factors from a list of many potential ones. Therefore, any experimental design shall be specified as a screening model if its primary purpose is to distinguish significant effects.[28, 29]

The Taguchi method is broadly used in conventional and nonconventional manufacturing processes.[30] The Taguchi model of the experimental system is an efficient methodology for statistically modifying the crucial parameters used in the ES process to control the corresponding electrospun fiber diameters and morphology effectively.[31-34] Several studies showed that the solution concentration is the most influential factor affecting the mean fiber diameter in ES.[35, 36] Low polymer concentration and feed rate, comparatively high applied voltage with a wide distance between the collector and the needle are needed to produce beadless fibers with the thinnest diameter in the ES process. However, a low concentration of polymer solution may result in some droplet formation.[37-39] The differences in identifying the main factor, which controls the electrospinning process to produce thinner nanofiber are dependent on the polymer type and composite used in the studies. Most studies used different polymer solutions with different concentrations.[40, 41] Some of these studies proved that the voltage is the prime factor, while others showed that feed rate is the main factor in controlling the process. More studies showed that the working distance is the key factor of the ES process.[4, 42, 43] Therefore, there is no unified parameters model to control the ES process. In this study, we add more clarification to this debate using our unique 3-polymer system.

The study tested three water-soluble polymers at different ratios in the composite fibers. The physical parameters, such as density, electrical conductivity, viscosity, and surface tension of the

4

selected solutions, were measured. We analyzed the effects of processing parameters on the diameter of fibers in detail by Taguchi and Regression methods. The mathematical model generated from the regression is used to find the optimum parameters. The genetic algorithm, a well-established optimization technique, is applied to find the optimum parameter values from the mathematical model. Fourier transform infrared spectroscopy (FTIR) was used to verify the molecular contents of the composite fibers. The diameters of fibers were measured by using scanning electron microscopy (SEM).

2. Results and Discussion

2.1. Physical properties of solutions

ES process control parameters such as humidity, temperature, polymer solution feed rate, working distance, applied voltage, and solution properties such as viscosity, density, surface tension, and electrical conductivity affect the formation and properties of nanofibers.[44, 45] These parameters were recorded for each solution (Table 1 and S1, Supporting Information).

Fiber size and morphology are affected by solution viscosity in ES due to a direct correlation between viscosity and morphology of fibers. Therefore, solution viscosity is one of the primary causes of nanofibers' ideal morphology (beadless and homogenous).[44] Moreover, surface tension plays a vital role in the morphology and size of electrospun nanofibers. For high surface tension, fibers generated are heavily beaded, or fibers may not form. In contrast, lower surface tension causes greater fiber stretching since fewer forces are needed to overcome the surface tension.[46] The electrical conductivity of a polymer solution and the attenuating force helps to determine the diameter of the fibers prepared during ES.[47, 48]

5

Table 1. ES procedures for seven different PVA/PVP/PEO concentration ratios

PVA/PVP/PEO ratio (v/v/v)	Working distance (mm)	Flow rate (mL/h)	Voltage (kV)
2:2:1	100-150	0.1-0.5	15-32
2:1:1	150-180	0.2-0.25	26-32
4:1:1	120-180	0.1-0.5	20-28
4:2:0.5	180	0.2	23-29
4:1:0.5	180	0.1	20-30
4:2:0.2	180	0.2	23-30
4:1:0.2	180	0.1	20-25

2.2. Process conditions

The process control parameters, such as working distance, flow rate, and applied voltage, have an essential role in producing nanofibers by ES.[49] These parameters are used to obtain ideal fiber morphologies and sizes; therefore, the parameters for each sample were recorded in Table S2, Supporting Information. The working distances at 120, 150, and 180 mm; flow rates at 0.1, 0.3, and 0.5 mL/h; and applied voltages at 20, 24, and 28 kV were tested in the production process of PVA/PVP/PEO samples.

ES clearly shows that the diameter of nanofibers decreased by increasing the working distance between the needle and collector and decreasing the polymer solution feed rate.[50] Generally, the diameter of the nanofibers is small at the beginning and gets bigger after a definite point by increasing the applied voltage beyond a critical value. The initial decrease in the diameter of nanofibers is attributed to a higher degree of jet stretching in correlation with enhanced charge repulsion within the jet and a strong external electric field as a result of the increase in the applied voltage. Moreover, the Taylor cone changes and unstable streams form due to increased applied voltage, causing beaded fibers to form due to a higher degree of whipping instability. On the contrary, nanofibers were not formed at low voltage.[51-53]

6

2.3. Morphological characterization of nanofibers

SEM was performed for the morphological characterization of nanofibers. According to the morphological analysis of fibers, an increase in the PVP ratio of PVA/PVP/PEO composite resulted in more beaded fibers, the number of beads increased (PVA/PVP/PEO = 2:2:1 vs 2:1:1, v/v/v) (Figure 1A and 1B). It was found that morphology started to be more beaded and non-homogenous after an increase in PEO ratio, in the case of PVA/PVP ratio is 4:2 (v/v) (PVA/PVP/PEO = 4:2:0.2 vs 4:2:0.5, v/v/v) (Figure 1C and 1D) but the crucial cause of the fiber to be more beaded was PVA/PVP ratio. Therefore, the PVP ratio was decreased compared to PVA, and PVA/PVP ratio was optimized at 4:1 (v/v) ratio in PVA/PVP/PEO composite fibers. This is to observe the irregular distribution of PVP in the PVA matrix with their weak interactions and with increasing PVP ratio in the PVA/PVP composites.[54] Then PEO was maximized in a similar ratio with the other polymers in the composite to observe the characteristic features of PEO. 0.2 and 1 volume ratio in the composite (PVA/PVP/PEO = 4:1:0.2, 4:1:0.5, and 4:1:1, v/v/v) proved to be beneficial. Over 1 volume ratio of PEO, in the case of PVA/PVP ratio is 4:1 (v/v), caused the fiber to be more beaded and non-homogenous, but between 0.2 and 1 ratios beadless morphologies were obtained. Hence, to reflect the features of PEO at a maximum in the composite, the maximum ratio (1 volume ratio at 4:1 (PVA/PVP, v/v) ratio) for PEO was chosen.

7
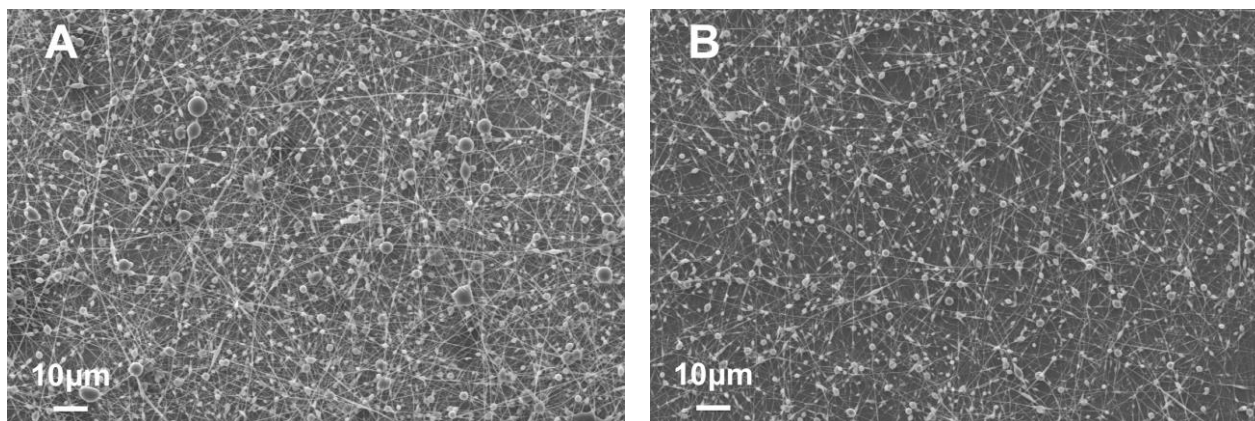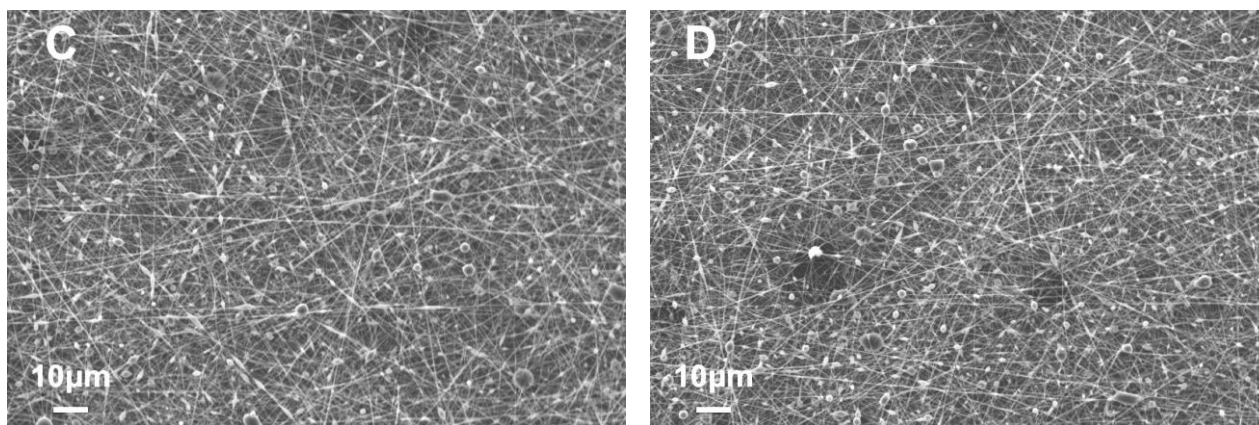
Figure 1. SEM images of PVA/PVP/PEO nanofibers at four ratios: (A) 2:2:1, (B) 2:1:1, (C) 4:2:0.2, and (D) 4:2:0.5.

The polymer ratio of PVA/PVP/PEO fibers was optimized at 4:1:1, v/v/v. In this ratio, twenty-one different process control parameter combinations were examined, and three samples for each parameter were produced. Thus, sixty-three samples were produced in the present study. The smallest diameter of fibers was obtained at 0.1 mL/h, 28 kV, and 180 mm, at a value $\varphi= 217\pm 42$ nm (Figure S1 C1-3, Supporting Information). The maximum diameter of fibers was produced at 0.5 mL/h, 20 kV, and 120 mm, at a value of $\varphi= 379 \pm 79$ nm (Figure S1 T1-3, Supporting Information). SEM images and fiber diameter distribution of three samples for each process combination are given in Figure 2.

2.4. Fiber composition

FTIR was used to analyze the molecular contents of nanofibers, and it proved that ES successfully produced PVA/PVP/PEO composite nanofibers. The molecular structures of pure PVA, PVP, and PEO and composite nanofiber fabricated by ES are given in Figure 2.

Pure PVP exhibits C-H asymmetric stretching bands at 2950.6 cm^{-1}, the characteristic amide C=O stretching vibration, which is the most intensive absorption band at 1645 cm^{-1}, CH$_2$ scissoring at 1492.6 cm^{-1}, C–N stretching vibrations at 1460.8 and 1421.3 cm^{-1}, C-H bending bands at 1372.1 and 1317.1 cm^{-1}, the characteristic absorption band of C–N stretching at 1286.3 cm^{-1}, and CH$_2$ twist

8

bands at 1228.4 and 1169.6 cm^{-1}. Also, O-H stretching vibrations band at 3403.7 cm^{-1} is caused by amide-iminol tautomerism.[55]

The inherent band of asymmetric (C-H) stretching of CH$_2$ shows absorption peaks of PEO at 2877.3 cm^{-1}. The peaks between 1342.2-1465.6 cm^{-1} and 1091.5 cm^{-1} are related to the swinging vibrations of C-H in the CH$_2$ group and the presence of the C-O-C stretching vibration of PEO, respectively. CH$_2$ rocking vibrations peaks at 956.5 and 839.8 cm^{-1} are caused by the methylene group and the helical structure.[56]

The large bands belong to the stretching O–H from the intermolecular and intramolecular hydrogen bonds are shown at 3271.6 cm^{-1}. The vibrational band of the stretching C–H from alkyl groups is observed at 2909.1 cm^{-1}. The peak at 1712.5cm^{-1} belongs to the stretching C=O and C–O from the acetate group remaining from PVA.[57]
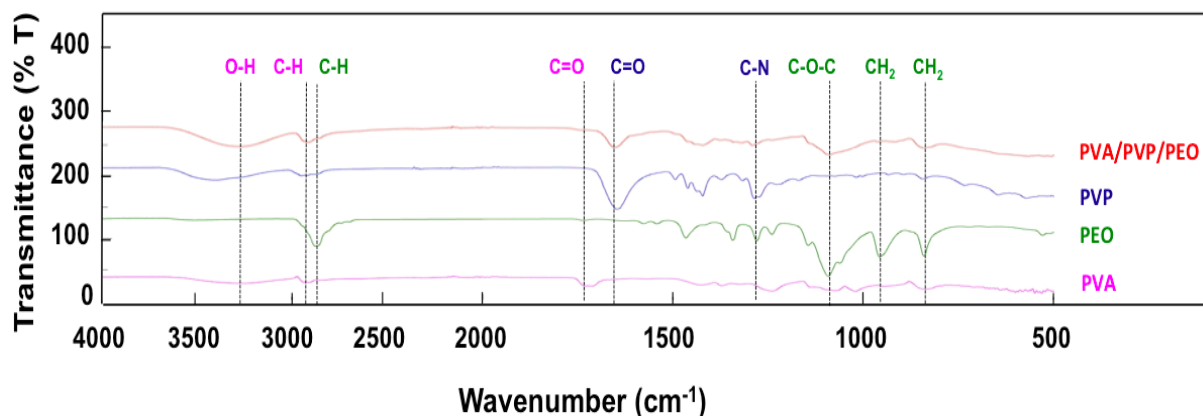
Figure 2. FTIR spectrums of pure PVA, PVP, PEO, and composite nanofiber samples.

2.5. Optimization of Nanofiber Diameters

The design of experiment (DOE) models are implemented in this study, namely Taguchi L$_9$, Taguchi L$_{27}$, and screening models, to form the experimental setup of producing nanofiber using the ES process. ANOVA is used to ratify the models with the regression method to deduce the mathematical model from the results. The study uses Minitab v19 software to analyze the models.

9

Later, the mathematical model is used by the optimization method, namely, the genetic algorithm (GA), to identify the optimum values of the ES process for the solution.

2.5.1. Taguchi Methods

The experimental variables are the flow rate, applied voltage, and working distance between the nozzle and collector of the ES system. The orthogonal matrices used are the L_9 and L_{27}, consisting of three variables with three levels, as shown in Table 2 and Table 5. Moreover, the screening model was applied, which confirms the results of the two Taguchi models.

Table 1. Experimental layout using L_9 orthogonal array of Taguchi method at the ratio of PVA/PVP/PEO (4:1:1, v/v/v)

	Samples	Electrospinning Process Parameters			Fiber Diameter (nm)
		Flow rate (mL/h)	Applied voltage (kV)	Working distance (mm)	
1	A	0.1	20	120	322 ± 16
2	B	0.1	24	150	267 ± 4
3	C	0.1	28	180	217 ± 7
4	D	0.3	20	120	333 ± 6
5	E	0.3	24	150	277 ± 5
6	F	0.3	28	180	231 ± 8
7	G	0.5	20	150	327 ± 1
8	H	0.5	24	180	260 ± 11
9	I	0.5	28	120	343 ± 13

Typically, a rigorous parameter design aims to find the factor settings to reduce the uncertainty of results around some optimal target value. The Taguchi methods achieve that by a two-step optimization. The first step focuses on minimizing variability among parameters, and the second focuses on hitting the target. Therefore, the experiment's outcomes are analyzed to make sure the inconsistency between parameters is the minimum. Then the ANOVA process is used to verify the model reliability.

The results obtained from the suggested experimental parameter combinations are listed in Table 2 for the first model of the Taguchi method. The model consists of nine proposed experimental setups based on three levels to draw them near to the behavior of the ES process.

10

Figure 3A validated the model's tightness as the experimental results' error residual for the signal to noise ratios (smaller is better) is less than 0.15. Furthermore, the model's findings confirmed that the optimum parameters are 0.1 mL/h for flow rate, 28 kV for applied voltage, and 180 mm for the working distance, as shown in Figure 3B and Figure 3C.
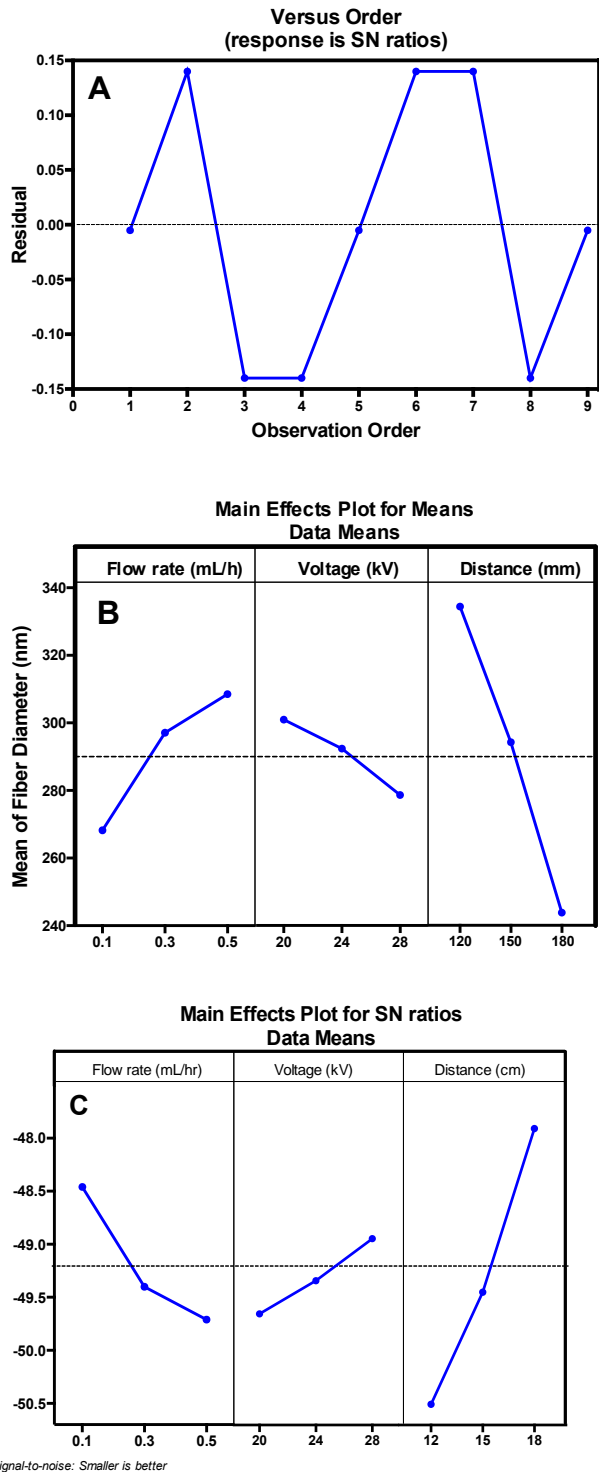
Figure 3. The response of the electrospinning parameters for L$_9$ Taguchi model: a) Error residuals, b) the effects of means of the parameters, and c) the effect of signal to noise ratios of the parameters.

11

In Table 3, the ranks in the response table identify that the working distance has the most significant influence on the diameter of fibers in ES compared to flow rate and applied voltage for this polymer solution. The Taguchi model was analyzed by the ANOVA method to verify the close-fitting of the model results, as shown in Table S3. The calculated R^2 is 0.992 ± 0.0025 (R^2 is a statistical measure of how close the data are to the fitted regression line with a value between 0 and 1, the higher the R^2, the better the model fits the data). The adjusted R^2 is 0.968 (adjusted R^2 is the modified version of R^2, which is adjusted for the number of variables in the model, adjusted R^2 is always less than R^2), which suggests the relation between parameters is so high, and therefore, the credibility of the model was proved.

Table 3. The response of means of L_9 orthogonal array of Taguchi method

Level	Flow rate (mL/h)	Voltage (kV)	Distance (mm)
1	268.2	301.7	335.2
2	297.1	293.0	294.7
3	308.5	279.1	243.8
Delta	40.3	22.6	91.4
Rank	2	3	1

Both Tables 3 and S4 use Delta to rank the factors according to their effects. Delta generally measures the extent of the effect by finding the difference between the average of the highest and lowest values for a specific element to identify the main factor among the experimental factors.

The second experimental process combinations were based on the Taguchi model L_{27} to analyze the ES process with more data. The analysis of L_{27} orthogonal array is identical to the L_9 orthogonal array, which reinforces the conclusion that working distance is the most influential variable. The outcome of the experimental process combinations was recorded in Table 4. It is worth mentioning that the results produced from the experiments have no significant variations

between the large fiber diameter sizes produced to the small fiber diameter sizes in contrast to the literature data that are opposite. The working distance has the most significant effect on the diameter of fibers, then the flow rate and final the applied voltage, respectively, in the ES process, as shown in Table S4.

P-value is the probability of measuring the results against the null hypothesis. Lower probabilities mean stronger proof against the null hypothesis. Generally, a significance level (referred to as α) of 0.05 is sufficient. For example, in Table S5, the P values for the applied voltage are 0.088 and 0.824 for 20 kV and 24 kV, respectively. In Table S6, the P-value is 0.122 for the applied voltage, which is higher than 0.05, and it is the limit for the effectiveness of the variable. However, P-value is 0.01 for the working distance and 0.046 for the flow rate, which is less than 0.05 (Table S6). These results demonstrated the significance of working distance as the major factor in controlling the size of the fiber diameter. The analysis of the Taguchi model is listed in Tables S7-8.

Table 4. Experimental Layout using L_{27} Orthogonal Array of Taguchi Method at the ratio of PVA/PVP/PEO (4:1:1, v/v/v)

	Samples	Electrospinning Process Parameters			Fiber Diameter (nm)
		Flow rate (mL/h)	Applied voltage (kV)	Working distance (mm)	
1	A1	0.1	20	120	299
2	A2	0.1	20	120	337
3	A3	0.1	20	120	329
4	B1	0.1	24	150	272
5	B2	0.1	24	150	261
6	B3	0.1	24	150	267
7	C1	0.1	28	180	210
8	C2	0.1	28	180	227
9	C3	0.1	28	180	214
10	M1	0.3	20	150	313
11	M2	0.3	20	150	317
12	M3	0.3	20	150	328
13	N1	0.3	24	180	245
14	N2	0.3	24	180	257
15	N3	0.3	24	180	247

13

16	O1	0.3	28	120	331
17	O2	0.3	28	120	327
18	O3	0.3	28	120	312
19	P1	0.5	20	180	264
20	P2	0.5	20	180	264
21	P3	0.5	20	180	266
22	Q1	0.5	24	120	378
23	Q2	0.5	24	120	353
24	Q3	0.5	24	120	356
25	R1	0.5	28	150	286
26	R2	0.5	28	150	292
27	R3	0.5	28	150	316

The R^2 value is again very high, which implies the trustworthiness of the Taguchi L_{27} model. In Table S8, the lowest P-value is for the working distance, and the second-lowest P-value belongs to the flow rate. However, the P-value for the applied voltage is higher than 0.05, indicating the variable's ineffectiveness to the ES of this composition. In Table 5, the Delta value ranks the variables (working distance, flow rate, and applied voltage), and the results are similar to the ranking in Table S4. It was also proved in Table S9 that the working distance has the most significant effect on the diameter of fibers and then flow rate and applied voltage, respectively, in the ES process. Therefore, both Tables 5 and S9 use Delta to rank the factors according to their effects.

Table 5. Response table for mean values

Level	Flow rate (mL/h)	Voltage (kV)	Distance (mm)
1	254.9	288.4	321.9
2	297.1	293.0	294.7
3	308.5	279.1	243.8
Delta	53.6	13.9	78.1
Rank	2	3	1

14
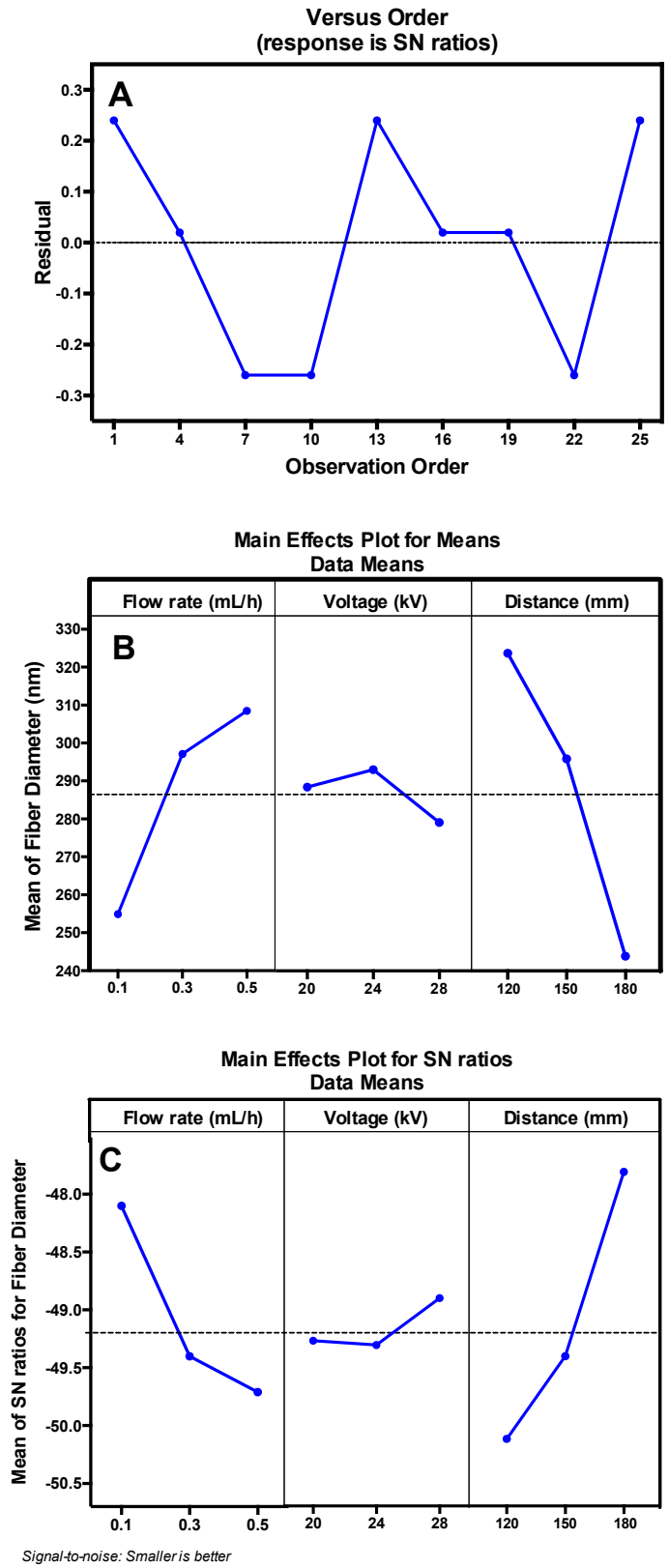
Figure 4. The response of the electrospinning parameters to the L_{27} Taguchi model: a) Error residuals, b) the effects of mean values of the parameters, and c) the effect of signal to noise ratios of the parameters.

In Figure 4, the behavior of L_{27} plots is similar to the plots of L_9 in which the optimum values to minimize the diameter of fibers are 0.1 mL/h for the flow rate, 28 kV for the applied voltage, and 180 mm for the working distance. Furthermore, the effects of means of the parameters are consistent with the effect of signal to noise ratios. Consequently, the results of L_{27} orthogonal matrices further consolidated the results of L_9 orthogonal matrices.

Figure 5 illustrates the actual experimental outcome with simulated results obtained from the equation for L_9 orthogonal array. Again, the two lines are almost identical, which support the utilization of the equation for any variable combinations.
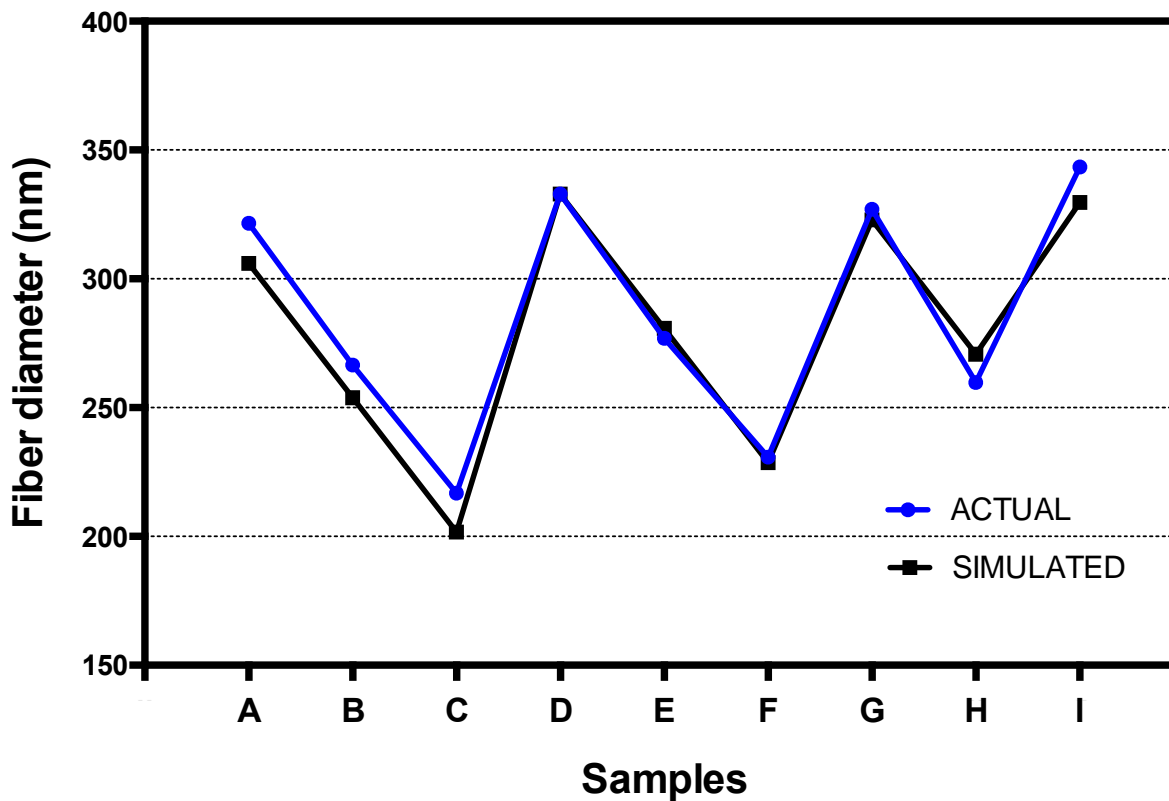
Figure 3. The actual and simulated fiber diameters in samples A-I.

2.5.2. Screening Method

Another DOE method, which is a screening model, was employed to test the two Taguchi models. The analysis results of the screening model match the ones of Taguchi. In Table S10, the R^2 is 0.918 ± 0.152 and the adjusted R^2 is 0.89, which again supports the implementation of the screening model as another DOE model. The P-value for the applied voltage is 0.012, which is higher than that for flow rate and working distance, as shown in Table S11. As shown in Figure 6, the three

16

variables have a higher value than the reference line (the red dotted line is the reference line showing which effects are statistically significant), which has a value of 2.26 but with different levels of effectiveness on the ES process. Here, the impact of the working distance on fiber diameter produced in the ES of the composition is higher than the flow rate and applied voltage.

In DOE, R^2 represents the percentage of variation in the response that is described by the method. Considering R^2 for the three methods, Taguchi L_9, Taguchi L_{27}, and Screening having values of 0.992 ± 0.0025, 0.973 ± 0.0044, and 0.918 ± 0.152, respectively, showing how reliable the results obtained from the experiments are. The value of R^2 decreases slightly from L_9 to L_{27} due to the increased number of experiments from L_9 to L_{27} with the same maximum and minimum values of the variables.
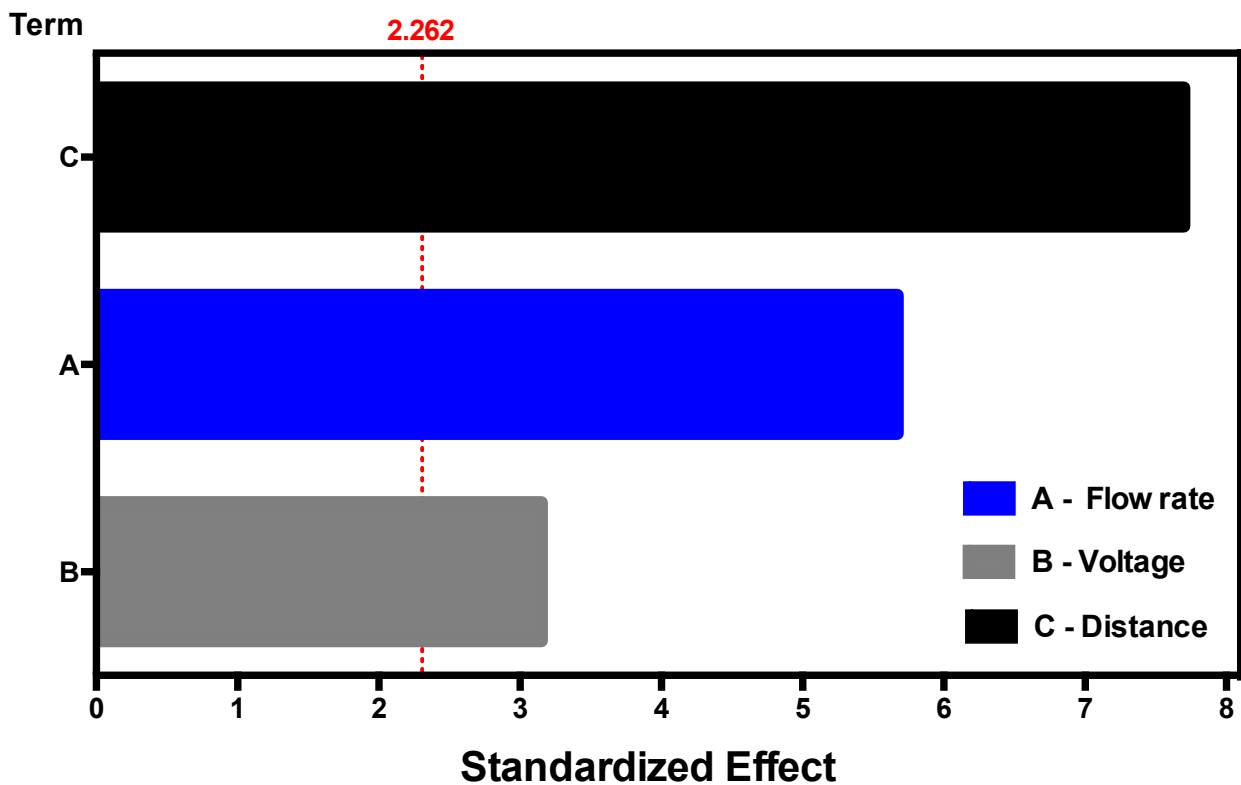
Figure 6. Pareto chart for the variable's effects as uncovered by the screening model.

2.5.3. Mathematical Model of Nanofiber Diameters

Based on the study's outcome, ANOVA has proved the trustworthiness of the DOE methods used in the current study, and a mathematical model was generated using regression analysis. The regression equation resulting from the analysis is:

$$\text{Fiber Diameter} = 516.2 + 134.8 \text{ x Flow rate} - 3.78 \text{ x Voltage} - 12.34 \text{ x Distance} \qquad (1)$$

The resulting equation from the analysis is of linear type, as shown in Figures 7A, B, and C. The plots are illustrated with an applied voltage of 20, 24, and 28kV. The plots show that the minimum fiber diameter is found at the lowest flow rate and the highest working distance.

(A)   (B)   (C)
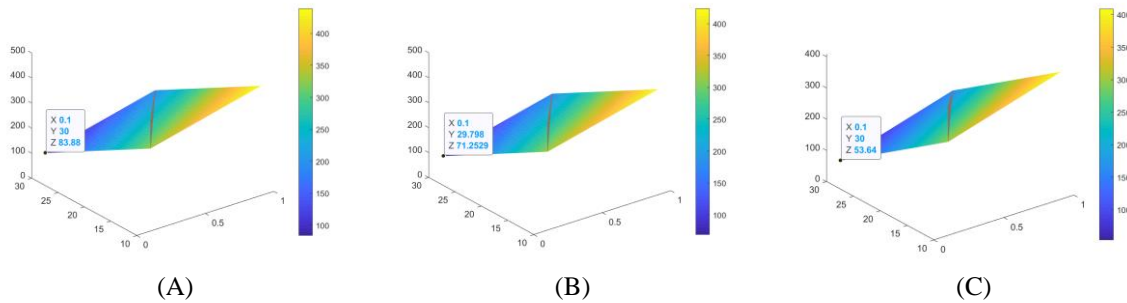
Figure 7. The plot of fiber diameter (equation 1) at applied voltage: A) 20 kV, B) 24kV, and C) 28kV.

2.5.4. Optimization of Nanofiber Diameters using Genetic Algorithm

The conclusions drawn from the above results pivoted the study's outcome in which the working distance between the tip of the needle and the collecting platform is the main parameter to control the fiber diameter produced by the ES of the composition's solution. As a result of the regression equation, the optimization algorithm was introduced to identify the optimum processing parameters for the required fiber diameter. The equation composes of three variables with one objective function. The study applies a genetic algorithm optimization method to equation (1) to find the optimum values of the ES process. The range for each variable is based on the operating machine limits, which are $0.001 \leq$ flow rate ≤ 689 mL/h, $1 \leq$ voltage ≤ 30 kV, and $100 \leq$ distance ≤ 200 mm. The model is coded using the genetic algorithm toolbox in Matlab with the parameters

18

(Population type: double vector with size 50, Fitness scaling: Rank, Selection: Stochastic uniform, Mutation: Constraint dependent, Crossover: Constraint dependent). The optimum value found by genetic algorithm for the fiber diameter is 156 nm for flow rate = 0.001 mL/h, voltage= 30 kV, and working distance= 200 mm. Experiment are conducted with the same optimum variables found by the optimization method. The fiber diameter experimental value is 161 nm, and when compared to the simulated result, the match is excellent (Figure 8).
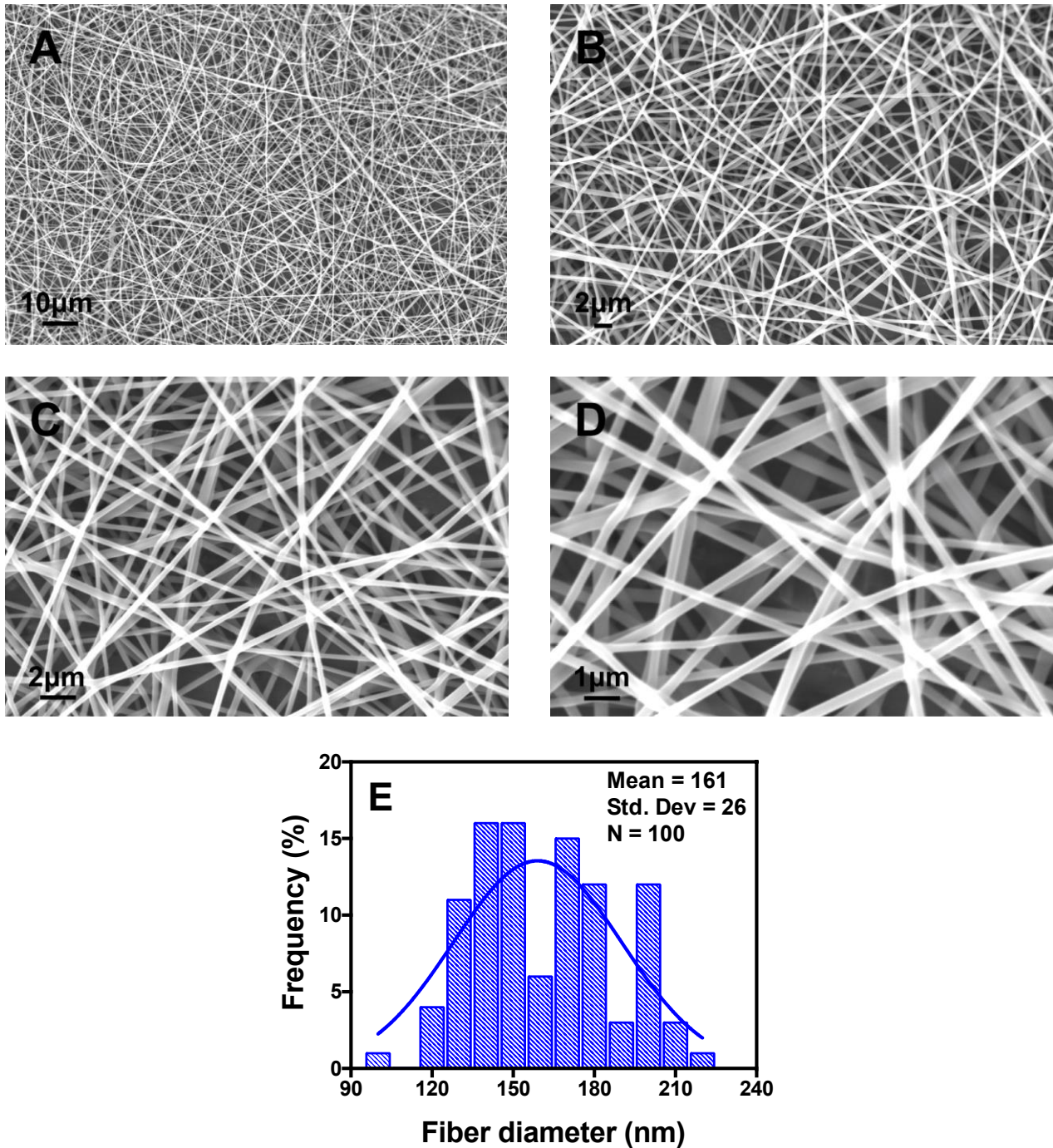
Figure 8. Fiber diameter distribution and SEM images with four different magnifications of the obtained PVA/PVP/PEO composite nanofibers with optimizing parameters (0.001 mL/h, 30 kV,

200 mm) set for the lowest diameter produced by the ES experimental setup. (a) 2k, (b) 5k, (c) 10k, (d) 20k magnification, and (e) fiber diameter distribution.

3. Conclusions

Several parameters can influence the ES process. Process-control parameters such as applied voltage, flow rate, and working distance significantly affect the morphology and diameter of fibers. The most used hydrophilic polymers, which have many advantages compared to other polymers such as non-toxic and non-carcinogenic features, were chosen, and polymeric PVA/PVP/PEO composite nanofibers were produced to verify the effect of these process-control parameters in the ES process. Taguchi and screening methods with regression has been used to evaluate the effect of these parameters on the diameter of fibers. The DOE methods used in the study to develop the experiments, Taguchi L_9, Taguchi $L_{27,}$ and Screening Method, showed their efficiency with R^2 values of 0.992, 0.973, and 0.918, respectively. These DOE methods are the epitome of such studies and provide rapid and reliable models for developing experiments. In future, our studies will explore using other DOE methods to design experiments of nanomanufacturing such as traditional DOE methods - Factorial, response surface, and new DOE methods such as Split plot design, Multi-stage split-plot (MSSP) design, Supersaturated design, and Mixture design. The results demonstrated the importance of working distance as a significant factor in controlling the size of the fiber diameter, in comparison to flow rate and applied voltage. In order to obtain fibers at the lowest diameter, fibers were produced with the optimized parameters, and it was found that the simulated result (156 nm) well matched the experimental value (161 nm).

4. Experimental Section

Materials: Polyvinyl pyrrolidone (PVP, Mw~ 40,000 g mol^{-1}), polyvinyl alcohol (PVA, Mw~89,000- 98,000 g mol^{-1} 99+% hydrolyzed), and polyethylene oxide (PEO, Mw~ average 600,000 g mol^{-1}) were obtained from Sigma-Aldrich (Poole, UK).

Preparation and characterization of solutions: The experiments were started with a solution having the same ratio for each polymer. PVA, PVP, and PEO were prepared at 15%, 15%,[58] and 4% w/v,[59] respectively, dissolving in distilled water. All solutions were dissolved separately, and PVA solution was mixed at $80\,^{o}$C for 1 hour. After that, PVA, PVP, and PEO complex solutions were mixed at seven different PEO/PVA/PVP concentrations (2:2:1, 2:1:1, 4:1:1, 4:2:0.5, 4:1:0.5, 4:2:0.2, and 4:1:0.2, respectively, v/v/v) in order to produce morphologically "ideal" nanofiber. The optimized polymer solution was selected at 4:1:1, v/v/v (PVA/PVP/PEO) ratio according to the results obtained using SEM.

Physical parameters such as density, viscosity, surface tension, and electrical conductivity for the solutions were measured by density bottle (10 mL specific density bottle, Boru Cam Inc., Turkey), viscometer (Brookfield DV-111, Harlow, UK), force tensiometer (Kruss K9, Hamburg, Germany), and electrical conductivity probe (Cond 3110 SET 1, WTW, Germany), respectively. All the measurements were performed three times at ambient temperature (25°C). These devices were calibrated before measurements.

Preparation and characterization of nanofibers: Initially, the PVA/PVP/PEO composition was set at seven different concentrations. ES was used to produce all these fibers at ambient temperature (25°C) and humidity (42%). Different ES parameters were used to produce nanofibers in these ratios to compare the size and morphology of nanofibers (Table 1). The different parameters (working distance, flow rate, and voltage) were selected according to the production of the nanofibers.

Scanning electron microscopy (SEM): The size and morphologies of nanofibers were examined with SEM (EVO LS 10, ZEISS). The surface of the samples was coated with gold for 60 seconds. The average fiber diameter and size distribution were ascertained by analyzing 100 fibers in randomly recorded SEM micrographs using software ImageJ (Brocken Symmetry Software).

Fourier transform infrared spectroscopy (FTIR): FTIR measurements were performed using a Jasco FT/IR 4700 spectrometer, and spectrographs were explicated using OPUS Viewer version 6.5

21

software. FTIR was used to analyse the molecular contents of nanofibers and confirm the presence of PVA, PVP, and PEO in the nanofibers. Measurements were obtained between 500 and 4000 cm^{-1} wavenumbers with a resolution of 4 cm^{-1} at 25 °C.

Statistical Analysis: SEM results are presented as mean ± standard deviation. Data analysis was performed using OriginPro 7.0 software (OriginLab Corporation, MA, USA).

Supporting Information

Supporting information is available from the Wiley Online Library or from the author.

Conflict of Interest

The authors declare no conflict of interest.

Keywords

Nanocomposites; electrospinning; numerical analysis; processing parameters

References

[1] X. Hong, S. Mahalingam, M. Edirisinghe, *Macromol. Mater. Eng.* **2017**, *302*, 1600564.

[2] L. T. H. Nguyen, S. Chen, N. K. Elumalai, M. P. Prabhakaran, Y. Zong, C. Vijila, S. I. Allakhverdiev, S. Ramakrishna, *Macromol. Mater. Eng.* **2013**, *298*, 822.

[3] R. Rasouli, A. Barhoum, M. Bechelany, A. Dufresne, *Macromol. Biosci.* **2019**, *19*, e1800256.

[4] J. Xue, T. Wu, Y. Dai, Y. Xia, *Chem. Rev.* **2019**, *119*, 5298.

[5] S. Soltani, N. Khanian, T. S. Y. Choong, U. Rashid, *New J. Chem.* **2020**, *44*, 9581.

[6] M. E. Cam, B. Ertas, H. Alenezi, A. N. Hazar-Yavuz, S. Cesur, G. S. Ozcan, C. Ekentok, E. Guler, C. Katsakouli, Z. Demirbas, D. Akakin, M. S. Eroglu, L. Kabasakal, O. Gunduz, M. Edirisinghe, *Mater. Sci. Eng. C* **2021**, *119*, 111586.

[7] O. Akampumuza, H. Gao, H. Zhang, D. Wu, X.-H. Qin, *Macromol. Mater. Eng.* **2018**, *303*, 1700269.

[8] W. Zhang, Z. He, Y. Han, Q. Jiang, C. Zhan, K. Zhang, Z. Li, R. Zhang, *Compos. Part A Appl. Sci. Manuf.* **2020**, *137*, 106009.

[9] K. Sarkar, C. Gomez, S. Zambrano, M. Ramirez, E. de Hoyos, H. Vasquez, K. Lozano, *Mater. Today* **2010**, *13*, 12.

[10] R. T. Weitz, L. Harnau, S. Rauschenbach, M. Burghard, K. Kern, *Nano Lett.* **2008**, *8*, 1187.

[11] J. Song, Z. Li, H. Wu, *ACS Appl. Mater. Interfaces* **2020**, *12*, 33447.

[12] C. Liu, B. Li, X. Mao, Q. Zhang, R. Sun, R. H. Gong, F. Zhou, *Macromol. Mater. Eng.* **2019**, *304*, 1900089.

[13] A. Baji, Y.-W. Mai, S.-C. Wong, M. Abtahi, P. Chen, *Compos. Sci. Technol.* **2010**, *70*, 703.

[14] R. S. Bhattarai, R. D. Bachu, S. H. S. Boddu, S. Bhaduri, *Pharmaceutics* **2018**, *11*, 5.

[15] P. Muthiah, T. J. Boyle, W. Sigmund, *Macromol. Mater. Eng.* **2013**, *298*, 1251.

[16] D. H. Reneker, A. L. Yarin, *Polymer* **2008**, *49*, 2387.

[17] R. L. Dahlin, F. K. Kasper, A. G. Mikos, *Tissue Eng. Part B Rev.* **2011**, *17*, 349.

[18] S. Jiang, Y. Chen, G. Duan, C. Mei, A. Greiner, S. Agarwal, *Polym. Chem.* **2018**, *9*, 2685.

[19] X. Yang, J. Wang, H. Guo, L. Liu, W. Xu, G. Duan, *e-Polymers* **2020**, *20*, 682.

[20] S. Agarwal, S. Jiang, Y. Chen, *Macromol. Mater. Eng.* **2019**, *304*, 1800548.

[21] T. S. Gaaz, A. B. Sulong, M. N. Akhtar, A. A. H. Kadhum, A. B. Mohamad, A. A. Al-Amiery, *Molecules* **2015**, *20*, 22833.

[22] V. G. Kadajji, G. V. Betageri, *Polymers* **2011**, *3*.

[23] F.-M. Chen, X. Liu, *Prog. Polym. Sci.* **2016**, *53*, 86.

[24] C. J. Luo, M. Nangrejo, M. Edirisinghe, *Polymer* **2010**, *51*, 1654.

[25] H. C. Oyeoka, C. M. Ewulonu, I. C. Nwuzor, C. M. Obele, J. T. Nwabanne, *J. Bioresources Bioproducts* **2021**, *6*, 168.

[26] J. Chen, X. Li, Q. Liu, Y. Wu, L. Shu, Z. He, C. Ye, M. Ma, *J. Biomed. Mater. Res. A* **2021**, *109*, 1468.

[27] A.-J. Shie, K.-H. Lo, W.-T. Lin, C.-W. Juan, Y.-T. Jou, *Biomed. Eng. Online* **2019**, *18*, 78.

[28] R. N. Kacker, E. S. Lagergren, J. J. Filliben, *J. Res. Natl. Inst. Stand. Technol.* **1991**, *96*, 577.

[29] L. M. Collins, J. J. Dziak, R. Li, *Psychol. Methods* **2009**, *14*, 202.

[30] R. Sureban, V. N. Kulkarni, V. N. Gaitonde, *Mater. Today* **2019**, *18*, 3034.

[31] N. A. S. Gundogdu, Y. Akgul, A. Kilic, *Aerosol Sci. Tech.* **2018**, *52*, 515.

[32] A. Nazir, N. Khenoussi, L. Schacher, T. Hussain, D. Adolphe, A. H. Hekmati, *RSC Adv.* **2015**, *5*, 76892.

[33] M. Elkasaby, H. A. Hegab, A. Mohany, G. M. Rizvi, *Adv. Polym. Tech.* **2018**, *37*, 2114.

[34] H. E. Abdelhakim, A. Coupe, C. Tuleu, M. Edirisinghe, D. Q. M. Craig, *Mol. Pharm.* **2019**, *16*, 2557.

[35] Y. Zheng, N. Meng, B. Xin, *Polymers* **2018**, *10*, 842.

[36] A. S. Motamedi, H. Mirzadeh, F. Hajiesmaeilbaigi, S. Bagheri-Khoulenjani, M. Shokrgozar, *Prog. Biomater.* **2017**, *6*, 113.

[37] V. Beachley, X. Wen, *Mater. Sci. Eng. C Mater Biol. Appl.* **2009**, *29*, 663.

[38] A. Hadjizadeh, H. Savoji, A. Ajji, *Biomed. Res. Int.* **2016**, *2016*, 8921316.

[39] Y. Duan, L. Kalluri, M. Satpathy, *J. Oral Biol.* **2021**, 1.

[40] A. Ahmadian, A. Shafiee, N. Aliahmad, M. Agarwal, *Textiles* **2021**, *1*.

[41] S. M. Feng, X. L. Liu, J. Qi, D. L. Huang, Z. C. Xiong, *Mater. Res. Express* **2019**, *6*, 125330.

[42] P. P. Mehta, V. S. Pawar, "22 - Electrospun nanofiber scaffolds: Technology and applications", in *Applications of Nanocomposite Materials in Drug Delivery*, Inamuddin, A.M. Asiri, and A. Mohammad, Eds., Woodhead Publishing, 2018, p. 509.

[43] E. Guler, Y. E. Baripoglu, H. Alenezi, A. Arikan, R. Babazade, S. Unal, G. Duruksu, F. S. Alfares, Y. Yazir, F. N. Oktar, O. Gunduz, M. Edirisinghe, M. E. Cam, *Int. J. Biol. Macromol.* **2021**, *190*, 244.

[44] R. M. Nezarati, M. B. Eifert, E. Cosgriff-Hernandez, *Tissue Eng. Part C Methods* **2013**, *19*, 810.

[45] A. Haider, S. Haider, I.-K. Kang, *Arab. J. Chem.* **2018**, *11*, 1165.

[46] H. Fong, I. Chun, D. H. Reneker, *Polymer* **1999**, *40*, 4585.

[47] R. S. Bhattarai, R. D. Bachu, S. H. S. Boddu, S. Bhaduri, *Pharmaceutics* **2019**, *11*.

[48] K. F. N. Cruz, E. C. Botelho, F. H. Cristovan, L. M. Guerrini, *Polymer Bulletin* **2017**, *74*, 2905.

[49] M. E. Cam, A. Nur Hazar-Yavuz, S. Cesur, O. Ozkan, H. Alenezi, H. Turkoglu Sasmazel, M. Sayip Eroglu, F. Brako, J. Ahmed, L. Kabasakal, G. Ren, O. Gunduz, M. Edirisinghe, *Int. J. Pharm.* **2020**, 119782.

[50] A. K. Maurya, P. L. Narayana, A. G. Bhavani, H. Jae-Keun, J.-T. Yeom, N. S. Reddy, *J. Electrostat.* **2020**, *104*, 103425.

[51] V. Pillay, C. Dott, Y. E. Choonara, C. Tyagi, L. Tomar, P. Kumar, L. C. du Toit, V. M. K. Ndesendo, *J. Nanomater.* **2013**, *2013*, 22.

[52] M. E. Cam, S. Cesur, T. Taskin, G. Erdemir, D. S. Kuruca, Y. M. Sahin, L. Kabasakal, O. Gunduz, *Eur. Polym. J.* **2019**, *120*, 109239.

[53] M. E. Cam, M. Crabbe-Mann, H. Alenezi, A. N. Hazar-Yavuz, B. Ertas, C. Ekentok, G. S. Ozcan, F. Topal, E. Guler, Y. Yazir, M. Parhizkar, M. Edirisinghe, *Eur. Polym. J.* **2020**, *134*, 109844.

[54] N. M. Deghiedy, S. M. El-Sayed, *Opt. Mater.* **2020**, *100*, 109667.

25

[55] M. E. Cam, S. Yildiz, H. Alenezi, S. Cesur, G. S. Ozcan, G. Erdemir, U. Edirisinghe, D. Akakin, D. S. Kuruca, L. Kabasakal, O. Gunduz, M. Edirisinghe, *J. R. Soc. Interface* **2020**, *17*, 20190712.

[56] H. T. Ahmed, O. G. Abdullah, *Polymers* **2019**, *11*, 853.

[57] A. M. Abd El-aziz, A. El-Maghraby, N. A. Taha, *Arab. J. Chem.* **2017**, *10*, 1052.

[58] D. Wang, J. Wang, *Chem. Eng. J.* **2017**, *314*, 714.

[59] H. Avci, R. Monticello, R. Kotek, *J. Biomater. Sci. Polym. Ed.* **2013**, *24*, 1815.

SEM images in higher resolution are available for Figure S1, which
were uploaded as Production Data in attached files, but I couldn't

Click here to access/download
Supporting Information
Optimization Supporting Information-MME_R1.docx

Click here to access/download
Production Data
Figure 1A.png

Click here to access/download
Production Data
Figure 1B.png

Click here to access/download
Production Data
Figure 1C.png

Click here to access/download
Production Data
Figure 2.png

Click here to access/download

Production Data

Figure 3B.png

Click here to access/download
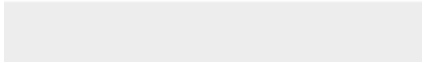**Production Data**
Figure 3C.png
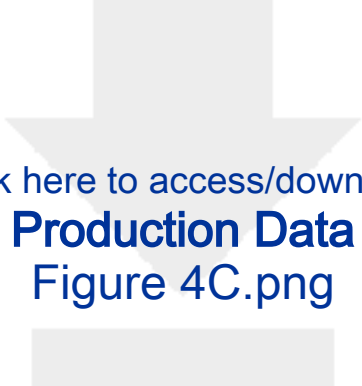
Click here to access/download
Production Data
Figure 4A.png
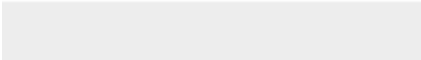
Click here to access/download
Production Data
Figure 4B.png
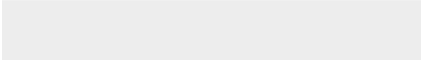
Click here to access/download

Production Data

Figure 4C.png
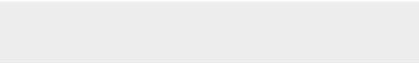
Click here to access/download
Production Data
Figure 5.png

Click here to access/download

Production Data

Figure 6.png

Click here to access/download

Production Data

Figure 7A.png

Click here to access/download
Production Data
Figure 7B.png

Click here to access/download
Production Data
Figure 7C.png

Click here to access/download

Production Data

Figure 8A.png

Click here to access/download
Production Data
Figure 8B.png

Click here to access/download
Production Data
Figure 8C.png

Click here to access/download

Production Data
Figure 8D.png

Click here to access/download

Production Data

Figure 8E.png
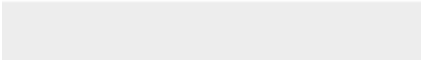
Click here to access/download
Production Data
Figure SA1.png

For Supporting Information
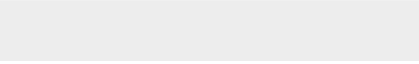
Click here to access/download
Production Data
Figure SA2.png
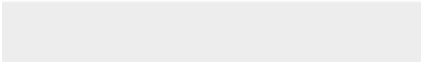
Click here to access/download
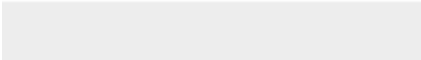**Production Data**
Figure SA3.png

Click here to access/download
Production Data
Figure SB1.png

Click here to access/download
Production Data
Figure SB2.png

Click here to access/download
Production Data
Figure SB3.png

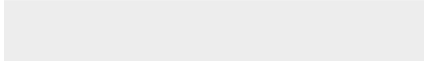For Supporting Information

Click here to access/download
Production Data
Figure SC1.png

For Supporting Information

Click here to access/download
Production Data
Figure SC2.png

Click here to access/download
Production Data
Figure SC3.png

For Supporting Information

Click here to access/download
Production Data
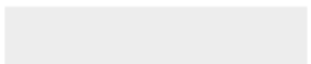Figure SD1.png

For Supporting Information
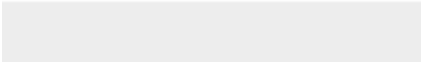
Click here to access/download
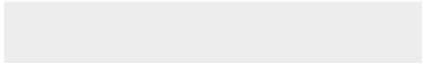**Production Data**
Figure SD2.png

Click here to access/download
Production Data
Figure SD3.png
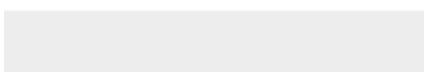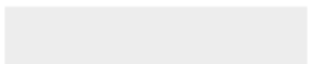
Click here to access/download

Production Data

Figure SE1.png
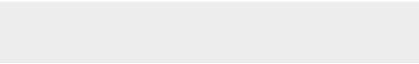
Click here to access/download
Production Data
Figure SE2.png

Click here to access/download
Production Data
Figure SE3.png

Click here to access/download
Production Data
Figure SF1.png
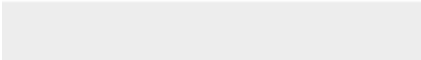
Click here to access/download
Production Data
Figure SF2.png

Click here to access/download
Production Data
Figure SF3.png

Click here to access/download
Production Data
Figure SG1.png

For Supporting Information

Click here to access/download
Production Data
Figure SG2.png

Click here to access/download
Production Data
Figure SG3.png
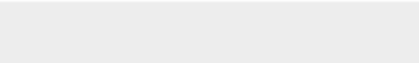
Click here to access/download
Production Data
Figure SH1.png
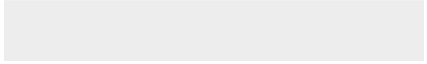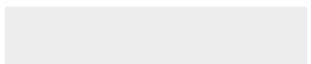
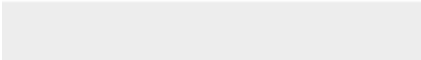Click here to access/download
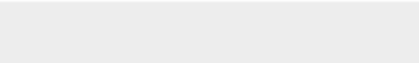**Production Data**
Figure SH2.png

Click here to access/download
Production Data
Figure SH3.png

For Supporting Information

Click here to access/download
Production Data
Figure SI1.png
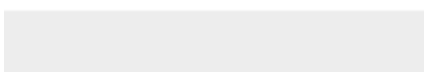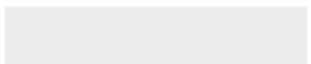
Click here to access/download
Production Data
Figure SI2.png
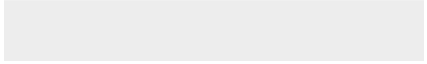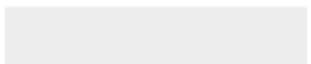
Click here to access/download
Production Data
Figure SI3.png
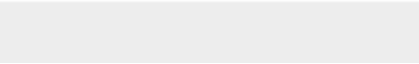
Click here to access/download
Production Data
Figure SJ1.png
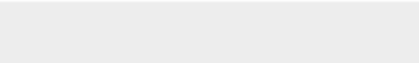
Click here to access/download
Production Data
Figure SJ2.png

Click here to access/download
Production Data
Figure SJ3.png

Click here to access/download
Production Data
Figure SK1.png

For Supporting Information

Click here to access/download
Production Data
Figure SK2.png

Click here to access/download
Production Data
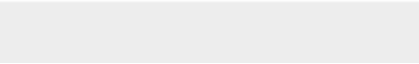Figure SK3.png
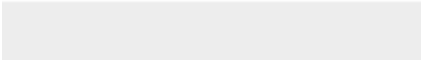
Click here to access/download
Production Data
Figure SL1.png
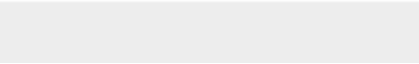
Click here to access/download
Production Data
Figure SL2.png

Click here to access/download
Production Data
Figure SL3.png

Click here to access/download
Production Data
Figure SM1.png

Click here to access/download

Production Data

Figure SM2.png
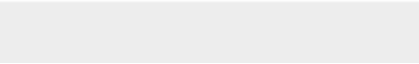
Click here to access/download

Production Data

Figure SM3.png

For Supporting Information

Click here to access/download
Production Data
Figure SN1.png

For Supporting Information

Click here to access/download
Production Data
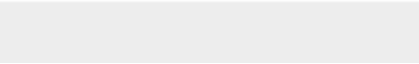Figure SN2.png

Click here to access/download
Production Data
Figure SN3.png

For Supporting Information

Click here to access/download
Production Data
Figure SO1.png

Click here to access/download

Production Data

Figure SO2.png

Click here to access/download
Production Data
Figure SO3.png

For Supporting Information

Click here to access/download
Production Data
Figure SP1.png

Click here to access/download
Production Data
Figure SP2.png

For Supporting Information

Click here to access/download
Production Data
Figure SP3.png

For Supporting Information

Click here to access/download
Production Data
Figure SQ1.png

Click here to access/download
Production Data
Figure SQ2.png

Click here to access/download
Production Data
Figure SQ3.png

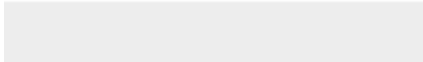For Supporting Information
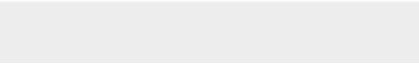
Click here to access/download
Production Data
Figure SR1.png

For Supporting Information

Click here to access/download
Production Data
Figure SR2.png

Click here to access/download
Production Data
Figure SR3.png

Click here to access/download
Production Data
Figure SS1.png

For Supporting Information

Click here to access/download
Production Data
Figure SS2.png

For Supporting Information

Click here to access/download
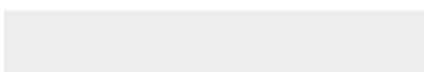**Production Data**
Figure SS3.png

Click here to access/download
Production Data
Figure ST1.png

Click here to access/download
Production Data
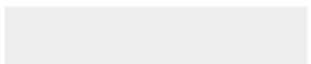Figure ST2.png

Click here to access/download
Production Data
Figure ST3.png

For Supporting Information

Click here to access/download
Production Data
Figure SU1.png

For Supporting Information

Click here to access/download
Production Data
Figure SU2.png

For Supporting Information

Click here to access/download
Production Data
Figure SU3.png